INSTITUTE OF PHYSICS PUBLISHING SMART MATERIALS AND STRUCTURES
Smart Mater. Struct. **12** (2003) 437–446 PII: S0964-1726(03)62188-9

Distributed optimal control of vibrations: a high frequency approximation approach

Mahamane Kader[1], **Michel Lenczner**[2] **and Zeljko Mrcarica**[3]

[1] Equipe de Mathématiques de Besançon, UMR 6623, Université de Franche-Comté, 16, Route de Gray, F-25030 Besançon Cedex, France
[2] Université Technologique de Belfort Montbéliard, F-90010 Belfort, France
[3] Laboratory of Electronic Design and Automation, Faculty of Electronic Engineering, Beogradska 14, 18000 Niš, Yugoslavia

Received 23 February 2001, in final form 4 November 2002
Published 14 May 2003
Online at stacks.iop.org/SMS/12/437

Abstract
This paper focuses on the design of distributed control related to distributed mechanical systems. The sensors and actuators are assumed to be numerous and periodically distributed. The problem addressed in this paper is: 'Can we find a way to approximate an optimal control law with a distributed electronic circuit for vibration reduction?'. Solutions to this problem are proposed in the framework of vibration control using piezoelectric actuators and sensors.

(Some figures in this article are in colour only in the electronic version)

1. Introduction

This paper is related to a distributed control problem arising in structural mechanics. Consider a thin beam covered on one side with a distribution of piezoelectric actuators and on the other side with piezoelectric sensors. Assume that this beam is subjected to either external forces or initial excitation. Our control objective is the optimal reduction of the vibration level.

The control strategy determination can be based on different theories. One of them, the optimal control theory, leads to an explicit expression of the control law. It has the advantage of being optimal with respect to a choice of functional that is minimized. Mathematical foundations of such a theory are well established and are also classical for many linear partial differential equations, see the comprehensive presentations of Curtain and Zwart [5], Bensoussan *et al* [2] and Lasiecka and Triggiani [6]. In practice, there is a strong limitation in the use of it for distributed control with many actuators and sensors. In fact, it produces a control law requiring that each actuator uses the data coming from every sensor. This constraint is generally unacceptable for realistic fabrication of distributed control systems. So, in practical applications, the active reduction of vibrations is performed with several single-input single-output (SISO) analog systems, that cannot implement an optimal control, or with one multiple-input multiple-output (MIMO) numeric system. It has now been realized that, due to time computation constraints, the size of such MIMO systems is limited and cannot be used for a large number of actuators and sensors.

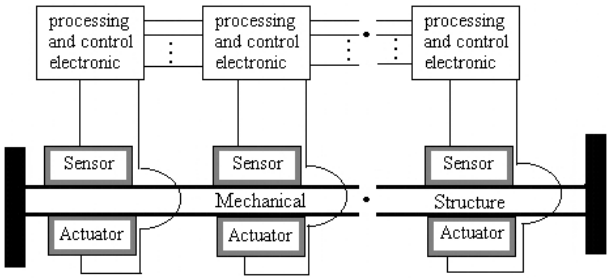

Figure 1. System including a distributed circuit.

The goal of this paper is to propose a new implementation of optimal control that does not suffer such a limitation. We show how the simplest optimal control strategy (linear quadratic regulator (LQR)) can be applied, in a realistic way, using a distributed electronic circuit. Each pair of actuator and sensor is only linked with its closest neighbors, see figure 1. The proposed solution is a kind of MIMO analog system. This approach, if applicable in reality, could cover the gap between cheap systems with limited efficiency (analog SISO) and expensive systems with good efficiency (numeric MIMO).

Let us remark that the problem of vibration control for a one-dimensional beam is quite simple and does not require a distribution of many actuators and sensors. However, this study is a preliminary investigation before considering more

complex cases of distributed control. Further interesting applications could be acoustic control or fluid flow control.

As already mentioned, we have implemented the simplest optimal control strategy, namely the LQR. In the future, application of more sophisticated control theory, including robust control, should be investigated.

Finally, the proposed solution could be extended by the use of numerical filters instead of analog ones. In this case, we will obtain a 'simplified' numeric MIMO instead of a 'complete' one. The required computation power will be less and then the possibility for numeric MIMO to deal with very large number of sensors and actuators will be extended significantly.

The paper is organized as follows. In section 2, the statement of the model and its reduction using asymptotic analysis is given. This simplified model is used in order to construct an optimal control law. The solution of the algebraic Riccati equation and its approximation with partial differential operators is given in section 3. Then, its approximation by distributed analog circuit is described in section 4. The last section is devoted to the numerical results.

2. Statement of the optimal control problem

We consider an elastic rectangular plate partially covered on both sides with piezoelectric transducers. Those located on the top are used as sensors while those located on the other face are actuators. The plate is assumed to be clamped on the two opposites sides Γ_0^a of the normal to the width direction and is free on the other parts of its boundary. The glued face of each piezoelectric transducer is connected to the earth. The upper face of each sensor is connected to the input of a current to current amplifier when the lower face of each actuator is connected to the output of an active voltage source.

2.1. The three-dimensional plate model

The motion of a multi-layered plate equipped with a distribution of piezoelectric transducers is characterized by the general electrodynamics equations for piezoelectric bodies. They can be found in [7]. Their weak form (or variational formulation) that has been derived in [4], for example, is composed of the weak form of the equation of dynamics:

$$\int_{\Omega^a}\left(\rho^a\sum_{i=1}^{3}\partial_{tt}^2 u_i^a v_i+\sum_{i,j=1}^{3}\sigma_{ij}^a s_{ij}(v)\right)\mathrm{d}x=0,$$

for all admissible displacement field $v \in V_{ad}^a$, where $V_{ad}^a = \{v = (v_i)_{i=1\ldots3} \in (H^1(\Omega^a))^3$ such that $v = 0$ on $\Gamma_0^a\}$ and the weak form of the equation of electrostatics: $\int_{\Omega^a}\sum_{i=1}^{3} D_i^a\partial_i\psi\,\mathrm{d}x = 0$, for all admissible electric potentials ψ (see [4]). Here $\Omega^a, a, x = (x_1, x_2, x_3), \partial_i, \partial_t, \rho^a, u^a, s_{ij}(v), \sigma^a, D^a$ and $H^1(\Omega^a)$ are, respectively, the domain occupied by the plate, its thickness, the coordinates in $\mathbb{R}^3$, the partial differential operators with respect to x_i and t, the volume mass, the vector of mechanical displacements, the strains $\frac{1}{2}(\partial_i v_j + \partial_j v_i)$, the mechanical stress tensor, the vector of electric displacements and the Sobolev space $\{v \in L^2(\Omega^a)$ such that $\partial_i v \in L^2(\Omega^a)$ for $i = 1\ldots3\}$. The other boundary conditions are not reported here (see [4] for details). Initial conditions are also not detailed here.

Mechanical stresses and electric displacements are assumed to be linearly dependent of the strain tensor $s_{kl}(u^a)$ and of the electric fields $\partial_k\phi^a$ (ϕ^a being the electric potential): $\sigma_{ij}^a = \sum_{k=1}^{3}(\sum_{l=1}^{3} R_{ijkl}s_{kl}(u^a) + e_{kij}\partial_k\phi^a)$ and $D_k^a = \sum_{j=1}^{3}(\sum_{i=1}^{3} e_{kij}s_{ij}(u^a) - c_{ki}\partial_i\phi^a)$, where R_{ijkl}, e_{kij} and c_{ki} are the stiffness, piezoelectric and permittivity tensors.

2.2. The two-dimensional thin plate model

In the following model formulation and in our simulation, the piezoelectric sensors and actuators are bonded symmetrically on the two faces of the elastic plate. The two-dimensional thin plate model considered in this section has been derived in [4] using an asymptotic method.

The motion equation for the two-dimensional model is given by

$$\int_{\omega}\rho\partial_{tt}^2 w v+\sum_{\alpha,\beta=1}^{2}\left(\sum_{\gamma,\delta=1}^{2} c_{\alpha\beta\gamma\delta}\partial_{\gamma\delta}^2 w+e_{\alpha\beta}\phi\right)\partial_{\alpha\beta}^2 v\,\mathrm{d}x=0 \quad (1)$$

for all admissible displacement $v \in V_{ad}$, with $V_{ad} = \{v \in H^2(\omega)$, such that $v = 0$ and $\sum_{\alpha=1}^{2}\partial_\alpha v n_\alpha = 0$ on $\Gamma_0 \subset \partial\omega\}$. Here $\omega, x = (x_1, x_2), \Gamma_0, n = (n_1, n_2), \rho, w, c_{\alpha\beta\gamma\delta}, e_{\alpha\beta}, \phi$ and $H^2(\omega)$ are the mean surface of the plate, the coordinates in $\mathbb{R}^2$, the boundary $\partial\omega$ where the plate is clamped, the vector normal to Γ_0 oriented to the exterior of ω, the surface mass, the transverse mechanical displacement, the bending stiffness tensor of the plate, the piezoelectric constant, the electric voltage on actuators and the Sobolev space $\{v \in L^2(\omega)$ such that $\partial_i v$ and $\partial_{ij} v \in L^2(\omega)$ for any $i, j = 1, 2\}$. The current flowing out of the upper surface S of a sensor, and measured with a current amplifier, is equal to

$$i^{sensor} = \sum_{\alpha,\beta=1}^{2} e_{\alpha\beta}\int_S \partial_{\alpha\beta t}^3 w\,\mathrm{d}s. \quad (2)$$

2.3. The homogenized one-dimensional beam model

Let us assume that sensors and actuators are numerous and periodically distributed on the plate. Thanks to homogenization theory, one may derive a simplified model of such a composite structure (see [3] for a rigorous presentation). It leads to a model of a homogeneous electro-mechanical medium, which presents a behavior close to the original one. Nevertheless the stiffness tensor, the piezoelectric strain and the permittivity matrix of this model are constants. Distributed continuous current and voltage model the currents flowing out of the sensor's upper surface and the actuator's voltages. The equations of the homogenized plate model are the same as (1) and (2). Only the value of the coefficients makes a difference. We do not introduce new notation for them; they are simply indexed by an H. This model is used for the optimal control synthesis.

We assume that the plate strains are pure bending in the direction ξ of the beam axis. It turns out that the strain in the other direction is small. Then the homogenized plate model can be replaced by a one-dimensional beam model:

$$\partial_{tt}^2 w + a\Delta^2 w + b\Delta\phi = 0 \qquad \text{on } (t, \xi) \in \mathbb{R}^+ \times \Omega, \quad (3)$$

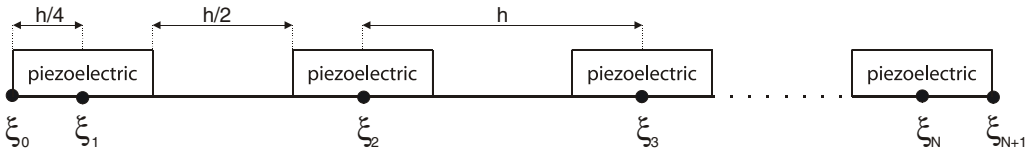

Figure 2. Coordinates $\xi_0, \ldots, \xi_{N+1}$.

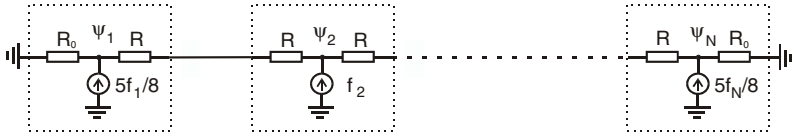

Figure 3. Realization of $\Delta_h \psi_h = I_h f_h$.

where $a = c^H_{1111}/\rho^H$ and $b = e^H_{11}/\rho^H$. Here, $\Omega =]0, L[$ and Δ is the one-dimensional Laplace operator: $\Delta = \partial^2_{\xi\xi}$. The boundary conditions are $w = \partial_\xi w = 0$ on $(t, \xi) \in \mathbb{R}^+ \times (\partial\Omega = \{0, L\})$. Initial conditions are chosen so that $w(0, \xi) = g(\xi)$ and $\partial_t w(0, \xi) = 0$, where g represents the displacements of the beam at $t = 0$. The density of current i delivered by the sensors is $i = e\Delta\partial_t w$ on $(t, \xi) \in \mathbb{R}^+ \times \Omega$, where $e = e^H_{11}$.

2.4. Optimal control

In the following, optimal control theory is applied to the one-dimensional homogeneous beam model. It is based on the general framework presented in [5]. We have chosen this approach because it is the simplest one developed for infinite-dimensional systems (in comparison with those of [2] and [6]) that can be applied for bounded control and observation operators.

First, let us write the model as a first-order system of differential equations:

$$\partial_t x = Ax + Bu \qquad \text{for } t > 0 \text{ and } x(0) = x^0. \tag{4}$$

Here the state variable $x = (w, \partial_t w)^t$ belongs to $L^2(\mathbb{R}^+; \mathcal{H})$, where $\mathcal{H} = H^2_0(\Omega) \times L^2(\Omega)$, $H^2_0(\Omega)$ being the set of functions w belonging to $H^2(\Omega)$ such that $w(t, \xi) = \partial_\xi w(t, \xi) = 0$ on the boundary $\mathbb{R}^+ \times \partial\Omega$. The scalar product on $\mathcal{H}$ is $((x_1, x_2), (y_1, y_2)) = \int_\Omega \partial^2_{\xi\xi} x_1 \partial^2_{\xi\xi} y_1 + x_2 y_2 \, \mathrm{d}\xi$. The control variable is $u = \phi$. The unbounded state operator $A : D(A) \subset \mathcal{H} \to \mathcal{H}$ is defined by $A = \begin{pmatrix} 0 & I \\ -aA_0 & 0 \end{pmatrix}$. It is densely defined on its domain $D(A) = H^4(\Omega) \cap H^2_0(\Omega) \times H^2_0(\Omega)$, where $A_0 = \Delta^2 = \partial^4_{\xi\xi\xi\xi}$, $H^2_0(\Omega) = \{v \in H^2(\Omega) \text{ so that } v = \mathrm{d}v/\mathrm{d}\xi = 0 \text{ on } \partial\Omega\}$. Its adjoint, in the sense of an adjoint of unbounded operators [5] (definition A.3.63, p 603), is $A^* = \begin{pmatrix} 0 & -aI \\ A_0 & 0 \end{pmatrix}$. It is also defined from $\mathcal{H}$ to $\mathcal{H}$ with $D(A^*) = D(A)$.

The bounded control operator $B : U = H^2(\Omega) \cap H^1_0(\Omega) \to \mathcal{H}$ is defined by $B = \begin{pmatrix} 0 \\ -b\Delta \end{pmatrix}$, where $H^1_0(\Omega) = \{v \in H^1(\Omega) \text{ so that } v = 0 \text{ on } \Gamma_0\}$. A straightforward calculation shows that the adjoint $B^* : \mathcal{H} \to U$ of B (see [5] definition A.3.57, p 601) is defined by $B^* x = (0, -b\Delta^{-1}) \begin{pmatrix} w \\ \partial_t w \end{pmatrix} = -b\Delta^{-1} x_2$. Consider a scalar c and the bounded observation operator $C : \mathcal{H} \to Y = H^2_0(\Omega)$ defined by $Cx = (\, cI \quad 0\,) \begin{pmatrix} w \\ \partial_t w \end{pmatrix} = cx_1 \in Y$.

Now, we consider the minimization problem: find $u \in L^2(\mathbb{R}^+; U)$ which minimizes the cost functional

$$J(u) = \int_0^\infty |Cx|^2_Y + |Du|^2_U \, \mathrm{d}t, \tag{5}$$

where the state variable x and the control variable u are constrained by the state equation (4). The bounded operator $D : U \to U$ is just multiplication by a constant $d > 0 : Du = du$.

Finally, $J(u)$ is equal to $\int_0^\infty \int_\Omega |c\partial^2_{\xi\xi} w|^2 + |d\partial^2_{\xi\xi} \phi|^2 \, \mathrm{d}\xi \, \mathrm{d}t$. Such choices for C and D were made so that it forces both the displacements x_1 and the control u to be regular, that is $\partial^2_{\xi\xi} w$ and $\partial^2_{\xi\xi} \phi$ belong to $L^2(\Omega)$. This is a guarantee for the safety of the mechanical structure as well as for the efficiency of the electronic circuit (prevention of local peaks in ϕ). Another criterion was on the decay rate (the real part of the exponent) of the modal amplitudes. With such a functional J, they are all the same. So, the efficiency of the resulting controller is uniformly distributed on all vibration modes.

It can be shown directly that (A, B) is exponentially stabilizable. This can be made by choosing one of the two stabilizing laws described in the following and by showing that the stabilized solution decays exponentially toward zero. This results in an explicit calculation. The same thing can be done for proving that (C, A) is exponentially detectable. So the minimization problem admits a unique solution. Following the optimal control theory, there exists a unique bounded nonnegative self-adjoint solution $X : \mathcal{H} \to \mathcal{H}$ to the algebraic Riccati equation:

$$(A^*X + XA - XB(D^*D)^{-1}B^*X + C^*C)x = 0, \quad \text{for all } x \in D(A) \tag{6}$$

and the optimal control u is given by

$$u = -(D^*D)^{-1}B^*Xx, \tag{7}$$

so the controlled equation is

$$\partial^2_{tt} w + a\Delta^2 w + b^2(X_{21} w + X_{22}\partial_t w) = 0 \quad \text{on } (t, \xi) \in \mathbb{R}^+ \times \Omega. \tag{8}$$

Remark 1. The velocity feedback, to which the optimal controller will be compared, $\phi = Ki = Ke\Delta\partial_t w$, with $K > 0$, leads to the exponentially stable system

$$\partial_{tt}^2 w + a\Delta^2 w + beK\Delta\partial_t w = 0 \qquad \text{on } \mathbb{R}^+ \times \Omega. \quad (9)$$

Since ϕ is a second-order derivative with respect to ξ, its value is proportional to the square of the spatial frequencies that are present in w. In practice such feedback leads to the saturation of the amplifiers and/or the actuators.

3. Exact solution X of the algebraic Riccati equation

In this section, we propose an approximation X_0 of the exact solution X. The derivation of X_0 is based on the expression of the exact solution X. Then, we detail the control law that is obtained when X is replaced by X_0. Since the state equation is a second-order one, X is a 2×2 matrix of operators $X = \begin{pmatrix} X_{11} & X_{12} \\ X_{21} & X_{22} \end{pmatrix}$.

Proposition 1. *The unique self-adjoint nonnegative solution of the algebraic Riccati equation (6) is given by*

$$X_{11} = \sqrt{2}\left(\frac{d}{b}\right)^2 a^{\frac{3}{2}}\left(-A_0 + A_0\left(I + \left(\frac{bc}{da}\right)^2 A_0^{-1}\right)^{1/2}\right)^{1/2} \times \left(I + \left(\frac{bc}{da}\right)^2 A_0^{-1}\right)^{1/2},$$

$$X_{12} = \left(\frac{d}{b}\right)^2 a\left(-I + \left(I + \left(\frac{bc}{da}\right)^2 A_0^{-1}\right)^{1/2}\right),$$

$$X_{21} = \left(\frac{d}{b}\right)^2 a\left(-A_0 + A_0\left(I + \left(\frac{bc}{da}\right)^2 A_0^{-1}\right)^{1/2}\right)$$

and

$$X_{22} = \sqrt{2a}\left(\frac{d}{b}\right)^2 a\left(-A_0 + A_0\left(I + \left(\frac{bc}{da}\right)^2 A_0^{-1}\right)^{1/2}\right)^{1/2}.$$

Proof. Its adjoint with respect to the scalar product $(\cdot,\cdot)_{\mathcal{H}}$ is also a bounded operator from $\mathcal{H}$ to $\mathcal{H}$ and given by $X^* = \begin{pmatrix} X_{11}^* & A_0^{-1}X_{21}^* \\ A_0X_{12}^* & X_{22}^* \end{pmatrix}$. Since the operator X is self-adjoint then $X_{11} = X_{11}^*$, $X_{22} = X_{22}^*$, $X_{12} = A_0^{-1}X_{21}^*$ and $X_{21} = A_0X_{12}^*$. Hence $X_{12} = X_{12}^*$ and $X_{21} = X_{21}^*$. So the equation $A^*X + XA - XB(D^*D)^{-1}B^*X + C^*C = 0$ is equivalent to

$$0 = \begin{pmatrix} c^2I & 0 \\ 0 & 0 \end{pmatrix} + \begin{pmatrix} 0 & -aI \\ A_0 & 0 \end{pmatrix}\begin{pmatrix} X_{11} & A_0^{-1}X_{21}^* \\ X_{21} & X_{22} \end{pmatrix} + \begin{pmatrix} X_{11} & A_0^{-1}X_{21}^* \\ X_{21} & X_{22} \end{pmatrix}\begin{pmatrix} 0 & I \\ -aA_0 & 0 \end{pmatrix} - \begin{pmatrix} X_{11} & A_0^{-1}X_{21}^* \\ X_{21} & X_{22} \end{pmatrix} \times \begin{pmatrix} 0 & 0 \\ 0 & (\frac{b}{d})^2 I \end{pmatrix}\begin{pmatrix} X_{11} & A_0^{-1}X_{21}^* \\ X_{21} & X_{22} \end{pmatrix},$$

which is equivalent to (where $\hat{b} = b/d$)

$$\begin{aligned} -aX_{21} - A_0^{-1}X_{21}^* aA_0 + c^2 I - \hat{b}^2 A_0^{-1}X_{21}^* X_{21} &= 0 \\ -aX_{22} + X_{11} - \hat{b}^2 A_0^{-1}X_{21}^* X_{22} &= 0 \\ A_0X_{11} - X_{22}aA_0 - \hat{b}^2 X_{22}X_{21} &= 0 \\ X_{21}^* + X_{21} - \hat{b}^2 X_{22}X_{22} &= 0. \end{aligned} \quad (10)$$

Since $X_{21} = X_{21}^*$ and commutes with A_0:

$$\hat{b}^2 A_0^{-1}X_{21}X_{21} + 2aX_{21} - c^2 = 0, \quad (11)$$

$$X_{11} = aX_{22} + \hat{b}^2 A_0^{-1}X_{21}X_{22}, \quad (12)$$

$$A_0X_{11} - X_{22}aA_0 - \hat{b}^2 X_{22}X_{21} = 0, \quad (13)$$

$$X_{22}^2 = \frac{2}{\hat{b}^2}X_{21}. \quad (14)$$

Equation (11) has two roots: $X_{21} = \frac{1}{\hat{b}^2}\left(-aA_0 \pm A_0\sqrt{a^2 + \hat{b}^2c^2A_0^{-1}}\right)$. From (14) X_{21} is nonnegative, so $X_{21} = \frac{a}{\hat{b}^2}\left(-A_0 + A_0\sqrt{I + \frac{\hat{b}^2c^2}{a^2}A_0^{-1}}\right)$. Since X is nonnegative, X_{22} is too, so from (14) and (12) we obtain successively $X_{22} = \sqrt{\frac{2a}{\hat{b}^4}\left(-A_0 + A_0\sqrt{I + \frac{\hat{b}^2c^2}{a^2}A_0^{-1}}\right)}$ and $X_{11} = \frac{\sqrt{2}a^{3/2}}{\hat{b}^2}\sqrt{-A_0 + A_0\sqrt{I + \frac{\hat{b}^2c^2}{a^2}A_0^{-1}}}\sqrt{I + \frac{\hat{b}^2c^2}{a^2}A_0^{-1}}$. Since $X_{12} = A_0^{-1}X_{21}$, then $X_{12} = \frac{a}{\hat{b}^2}\left(-I + \sqrt{I + \frac{\hat{b}^2c^2}{a^2}A_0^{-1}}\right)$.

Remark 2. It is worth looking at this exact solution. Since it is composed of square roots of partial differential operators, it is clearly a non-local operator. Implementation of such a control law using distributed circuits should require that any given actuator should receive measurements from all sensors. As was already explained in the introduction, this constraint is too strong for the fabrication of real systems. That is the reason why an approximation of X will be considered.

3.1. An approximation of X

An analysis of the algebraic Riccati equation shows that each component X_{ij} of X can be written as $X_{ij} = \sum_{k\in\mathbb{Z}} X_{ij,k}A_0^k$. We make a Taylor series expansion with respect to A_0^{-1}, for each component $X_{11} = \frac{cd\sqrt{a}}{b}I + \frac{bc^3}{2da^{\frac{3}{2}}}A_0^{-1} + o(A_0^{-1})$, $X_{12} = \frac{c^2}{2a}A_0^{-1} - \frac{b^2c^4}{8d^2a^3}A_0^{-2} + o(A_0^{-2})$, $X_{21} = \frac{c^2}{2a}I - \frac{b^2c^4}{8d^2a^3}A_0^{-1} + o(A_0^{-1})$ and $X_{22} = \frac{cd}{b\sqrt{a}}I - \frac{bc^3}{8a^{\frac{3}{2}}d}A_0^{-1} + o(A_0^{-1})$.

The following choice of an approximation X_0 of X is based on this series expansion, where only some terms are conserved. It insures that both the quality of the approximation and the stability of the homogenized model with this approximated controller are good enough:

$$X_0 = \begin{pmatrix} \frac{cd\sqrt{a}}{b}I + \frac{bc^3}{2a^{\frac{3}{2}}d}A_0^{-1} & \frac{c^2}{2a}A_0^{-1} \\ \frac{c^2}{2a}I & \frac{cd}{b\sqrt{a}}I \end{pmatrix}.$$

We readily see that the residual operator $Q(X_0) = A^*X_0 + X_0A - X_0BD^{-2}B^*X_0 + C^*C$ has the simple expression $Q(X_0) = \begin{pmatrix} -\frac{b^2c^4}{4d^2a^2}A_0^{-1} & 0 \\ 0 & 0 \end{pmatrix}$. The approximation error is given by the norm of the residual operator $\|Q(X_0)x\|_{\mathcal{H}} \leqslant \frac{b^2c^4}{4d^2a^2\lambda_1}\|x\|_{\mathcal{H}}$, where λ_1 is the first eigenvalue of A_0. This implies the next proposition.

Proposition 2. *$Q(X_0) \leqslant 0$ and the system (4) stabilized by $u = -D^{-2}B^*X_0x$ is exponentially stable.*

Now, replacing X by X_0 in (7), ϕ is the solution of the boundary value problem:

$$\Delta\phi = \frac{c}{d\sqrt{a}}\partial_t w + \frac{bc^2}{2d^2 a}w \qquad \text{in } \Omega \text{ and } \phi = 0 \text{ on } \partial\Omega. \tag{15}$$

By another way, from the sensor equation, $\partial_t w = w_t$ is the solution of

$$\Delta w_t = \frac{i}{e} \qquad \text{in } \Omega \text{ and } w_t = 0 \text{ on } \partial\Omega. \tag{16}$$

Using this equation, one can compute $\partial_t w$ and thus w by integration. Using (15), one can deduce ϕ. The resulting control law is derived by a cascade of equations involving only local operators. Thus, a distributed electronic circuit having connections only between neighbors can approximate it.

Introducing (15) in (3), it gives $\partial^2_{tt} w + a\Delta^2 w + \frac{bc}{d\sqrt{a}}\partial_t w + \frac{1}{2}(\frac{bc}{d\sqrt{a}})^2 w = 0$, or equivalently, with $d = \frac{bc}{2\sigma_0\sqrt{a}}$ (σ_0 denoting the decay rate of w):

$$\partial^2_{tt} w + a\Delta^2 w + 2\sigma_0\partial_t w + 2\sigma_0^2 w = 0. \tag{17}$$

4. Approximation by a distributed electronic circuit

The control law based on X or X_0 has been derived from the homogenized beam model. That is the reason why it is constituted with partial differential operators with constant coefficients. Evidently, this control law cannot be directly applied to a real system having a finite number of actuators and sensors. Now, we will discretize the cascade of equations constituting the controller. Then, a distributed circuit implementing the discretized controller will be described.

The centers of the N actuators (and the sensors) are denoted by $(\xi_n)_{n=1\ldots N}$. The distance between two actuators (or sensors) is denoted by h. Their length is equal to $\frac{h}{2}$. The centers of the first and the last actuators are located, respectively, at $\xi = \frac{h}{4}$ and $\xi = L - \frac{h}{4}$, so $(\xi_1, \xi_2, \ldots, \xi_N) = (\frac{h}{4}, (1+\frac{1}{4})h, \ldots, (N-\frac{3}{4})h)$ and $h = \frac{L}{N-\frac{1}{2}}$. This sequence is completed with the coordinates of the extremities $\xi_0 = 0$ and $\xi_{N+1} = L$.

The second-order finite difference discretization of the Laplace equation $-\Delta\psi = f$ in Ω, with Dirichlet boundary conditions $\psi = 0$ on the boundary $\xi \in \{0, L\}$ is

$$\begin{aligned}
&4\frac{\psi_1 - \psi_0}{2R} - \frac{\psi_2 - \psi_1}{2R} = \frac{5}{8}f_1,\\
&\frac{\psi_n - \psi_{n-1}}{2R} - \frac{\psi_{n+1} - \psi_n}{2R} = f_n \qquad \text{for } n \in \{2, \ldots, N-1\},\\
&\frac{\psi_N - \psi_{N-1}}{2R} - 4\frac{\psi_{N+1} - \psi_N}{2R} = \frac{5}{8}f_N,\\
&\psi_0 = \psi_{N+1} = 0,
\end{aligned}$$

where $R = \frac{h^2}{2}$, ψ_n and f_n being some approximations of $\psi(\xi_n)$ and $f(\xi_n)$. The factors 4 and $\frac{5}{8}$ are introduced in order to preserve the second order of the approximation scheme at the extremities. This set of equations is denoted by $\Delta_h\psi_h = I_h f_h$, where $\psi_h = (\psi_0, \ldots, \psi_{N+1})$ and $f_h = (f_1, \ldots, f_N)$. It can be solved using the distributed circuit represented in figure 3, $I_h f$ being its distributed input, ψ_h the potentials at the resistors nodes and $R_0 = R/2$.

The finite difference approximation of equation (16) is $\Delta_h w_{t,h} = \frac{1}{e} I_h i_h$, where $w_{t,h} = (w_{t,0}, \ldots, w_{t,N+1})$. The components of $i_h = (i_1, \ldots, i_N)$ are the means of the currents flowing from sensors: $i_n = \frac{i_n^{sensor}}{h} \approx \frac{1}{h}\int_{S_n} e_{11}\partial^2_{x_1x_1} w_{t,h}(x_1, x_2)\,\mathrm{d}x_1\,\mathrm{d}x_2$. So, i_h is an approximation of the current density i. Finally, the computation of $w_{t,h}$ is realized by the first layer of the circuit represented in figure 4, with amplification coefficients $k = \frac{1}{he}$ and $k^0 = \frac{5}{8}k$. Furthermore, the values of $w_h = (w_0, \ldots, w_{N+1})$ are derived by a temporal integration, using a capacitor so that $C = 1$.

The controller equation (15), with $d = \frac{bc}{2\sigma_0\sqrt{a}}$, is approximated in the same way by $\Delta_h\phi_h = \frac{2\sigma_0}{b} I_h\partial_t w_h + \frac{2\sigma_0^2}{b} I_h w_h$ and implemented by the second layer of the circuit in figure 4 with amplification coefficients $k_1 = \frac{2\sigma_0^2}{b}$, $k_2 = \frac{2\sigma_0}{b}$ and $k_i^0 = \frac{5}{8}k_i$ for $i \in \{1, 2\}$. Finally, we remark that, as has been announced in the introduction, each processing cell of the circuit communicates only with neighboring cells.

In another way, the electronic realization of the velocity feedback $\phi_h = K i_h$, or equivalently $(\phi_n = \frac{K}{h} i_n^{sensor})_{n\in\{1,\ldots,N\}}$, is represented in figure 5, where $K' = \frac{K}{h}$.

5. Numerical simulations

The numerical simulations have been carried out for a brass elastic plate. Its dimensions are 155 mm × 5 mm × 2 mm and it includes sixteen pairs of sensors/actuators. The sixteen pairs of square piezoelectric transducers are PZT ceramics, with dimensions 5 mm × 5 mm × 0.2 mm. So $L = 155$ mm and $h = 10$ mm.

Two series of simulations have been realized. They are based, respectively, on the homogenized model, with which an exact calculation is possible, and the two-dimensional thin plate model, which is solved using a finite element method. For both models, the velocity feedback and the optimal controller have been numerically implemented.

5.1. Exact solution of the homogenized model

The eigenvectors associated with the homogenized equation (3) are $(\psi_n \in H_0^2(\Omega))_{n\in\mathbb{N}^*}$ solutions of $a\frac{\mathrm{d}^4\psi_n}{\mathrm{d}\xi^4} - \lambda_n\psi_n = 0$ in Ω. Introducing the scaling $y = \frac{\xi}{L}$, the functions $\eta_n(y) = \psi_n(\xi)$ are the solutions of $\eta_n \in H_0^2(]0,1[)$ and $\frac{\mathrm{d}^4\eta_n}{\mathrm{d}y^4} - \mu_n^4\eta_n = 0$ in $]0,1[$, with μ_n so that $\lambda_n = a\frac{\mu_n^4}{L^4}$. The general solution can be written $\eta_n(\mu_n y) = As_1(\mu_n y) + Bc_1(\mu_n y) + Cs_2(\mu_n y) + Dc_2(\mu_n y)$, where $s_1(\mu_n y) = \sin(\mu_n y) + \sinh(\mu_n y)$, $c_1(\mu_n y) = \cos(\mu_n y) + \cosh(\mu_n y)$, $s_2(\mu_n y) = -\sin(\mu_n y) + \sinh(\mu_n y)$ and $c_2(\mu_n y) = -\cos(\mu_n y) + \cosh(\mu_n y)$. Taking into account the boundary conditions, it follows that μ_n is a solution of the transcendental equation $\cos\mu_n\cosh\mu_n - 1 = 0$ and $\eta_n(\mu_n\xi) = C(s_2(\mu_n y) - \frac{s_2(\mu_n)}{c_2(\mu_n)}c_2(\mu_n y))$. Finally, the eigenvectors ψ_n are deduced from the expression for η_n by descaling.

Furthermore, the solution $w(t, \xi)$ can be decomposed on the basis $\{\psi_n\}_{n\in\mathbb{N}^*}$ which is orthonormal for the $L^2(\Omega)$ scalar product: $w(t, \xi) = \sum_{n\in\mathbb{N}^*} w_n(t)\psi_n(\mu_n\xi)$.

Replacing w by its decomposition in (8), (17) and (9), it follows that w_n is a solution of

$$\partial^2_{tt} w_n + \lambda_n w_n + \frac{b^2}{d^2}(X_{21,n} w_n + X_{22,n}\partial_t w_n) = 0 \tag{18}$$

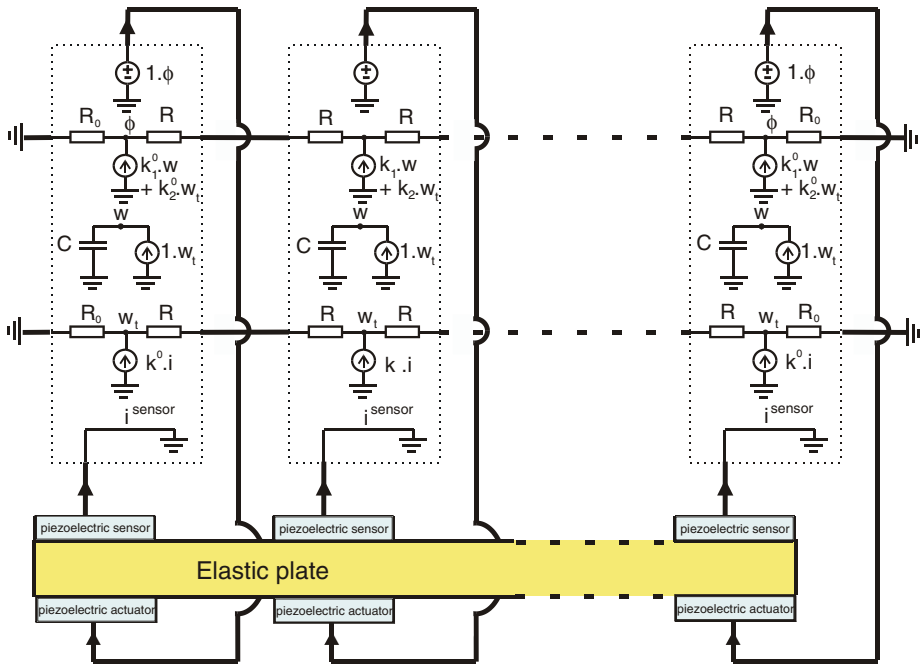

Figure 4. Realization of the optimal controller.

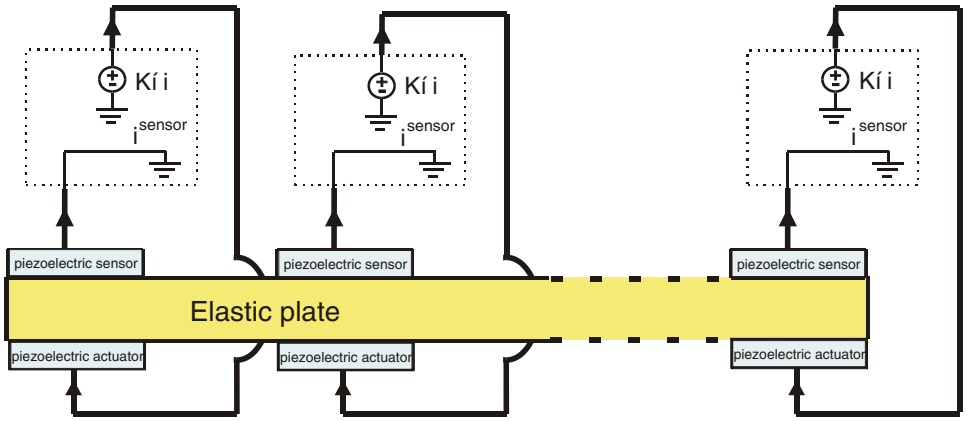

Figure 5. Realization of the velocity feedback.

in the optimal control case,

$$\partial_{tt}^2 w_n + \lambda_n w_n + 2\sigma_0 \partial_t w_n + 2\sigma_0^2 w_n = 0 \tag{19}$$

in the approximate optimal control case and

$$\partial_{tt}^2 w_n + \lambda_n w_n + eKb\lambda_n \partial_t w_n = 0 \tag{20}$$

in the velocity feedback case. In (18), $X_{21,n} = \left(\frac{d}{b}\right)^2\left(-\lambda_n + \lambda_n\sqrt{1+(bc)^2/(d^2a\lambda_n)}\right)$ and $X_{22,n} = \sqrt{2a}\left(\frac{d}{b}\right)^2 \sqrt{-\lambda_n + \lambda_n\sqrt{1+(bc)^2/(\lambda_n d^2 a)}}$ are the eigenvalues of X_{21} and X_{22} associated with the eigenfunction ψ_n, that is $X_{21}\psi_n = X_{21,n}\psi_n$ and $X_{22}\psi_n = X_{22,n}\psi_n$. In (20), the amplification coefficient K is chosen so that both controls, the velocity feedback and the optimal one, lead to the same decay rate of the first mode, that is $K = 2\sigma_0/eb\lambda_1$. So the equation with velocity feedback can be rewritten as

$$\partial_{tt}^2 w_n + \lambda_n w_n + \frac{\lambda_n}{\lambda_1} 2\sigma_0 \partial_t w_n = 0. \tag{21}$$

We have computed exact solutions of (18), (19) and (21). For the range of frequencies being studied here, the results of (18) and (19) are very similar, so only those of (18) and (21) are discussed in this paper.

5.2. The two-dimensional thin plate model

The two-dimensional thin plate model (1) is discretized using a finite element method. Thirty one elements are used in the longitudinal direction and one element in the other. Each of them are 5 mm × 5 mm in size, so each pair of piezoelectric transducers is discretized with only one element. The mechanical field w and the electrical potentials are discretized on each element by the twelve-node non-conformal Adini finite element and constant fields.

The global differential system associated to the mechanical structure and the distributed circuit is solved using the electronic circuit simulator Alecsis [1]. The electrical circuits and their connection with the mechanical structure

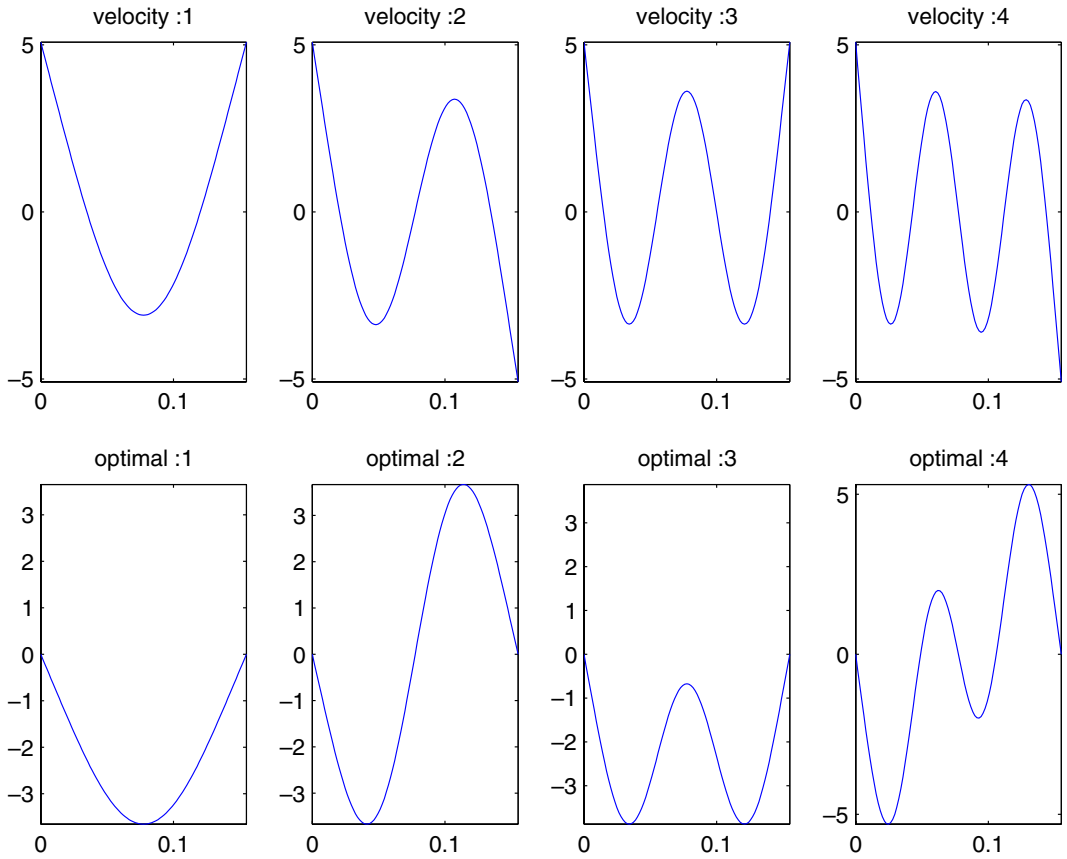

Figure 6. Voltage shapes.

are defined in Alecsis. The FE solver provides the mesh and elementary matrices. The files created by the FE processing program and the description of the electronic circuit are introduced in Alecsis. This last constructs the global matrices and solves the global differential system.

Simulations based on both circuits represented in figures 4 and 5 have been carried out using this FE circuit simulator. An explicit Euler scheme with 1024 time steps was used for time discretizations.

5.3. Numerical results

Before we discuss the results of the controlled systems, let us compare the two models. They are two different approximations of the same real system. The homogenized one is its asymptotic limit, for a vanishing size of the periodicity cell, while the other is just its finite element approximation. Comparisons are made on the time and space distribution of solutions. Eigenfrequencies are the major model characteristics for its temporal behaviour. They are denoted by f_{Hom} and f_{FEM} and compared in table 1, which shows a good agreement of the two models on this aspect. Quadratic norms of the difference of normalized eigenmodes ψ_n of the two models, which characterize spatial distributions of solutions, are in the fifth column of table 1. Since they are also very small, one can conclude that the two models behave similarly.

Further, spatial distribution of controllers must be compared. This is done in the sixth column of table 1, where $\bar{\phi}_n^{Hom}$ and $\bar{\phi}_n^{FEM}$ are the shapes, related to the mode number n, of the optimal control computed on the homogenized model and of the discretized approximate optimal control which is the output of the distributed circuit of figure 4.

Here, the error magnitudes are much higher. This is not surprising, because the computation of the approximate optimal control requires two successive discretized Laplace operator inversions, with discretization steps that are two times larger than those used in the FEM. Due to the relatively large error on the control shapes, an efficiency loss of the controller is possible.

The further investigation is on the effect of the two kinds of controls: the velocity feedback and the optimal control. As usual, the most important quantity to be discussed is the evolution of mechanical displacements. However, because our interest is highly oriented towards electronics integration in mechanical structures, severe restrictions on the size of devices and consequently on the voltage amplitudes to be imposed on actuators, must be considered. It is also useful to draw attention to the fact that, with such control synthesis, directly based on the partial differential equation and not on modal participations, the control effect is global. It takes place on every mode at the same time. For given excitations, the distribution of the controller amplitude, with respect to each mode, is determined only by the choice of the functional J (5). So, it cannot be driven mode by mode.

Having all these considerations in mind, we have adopted a functional J, see (5), which insures that the norm of the controller is reasonably bounded with respect to frequency

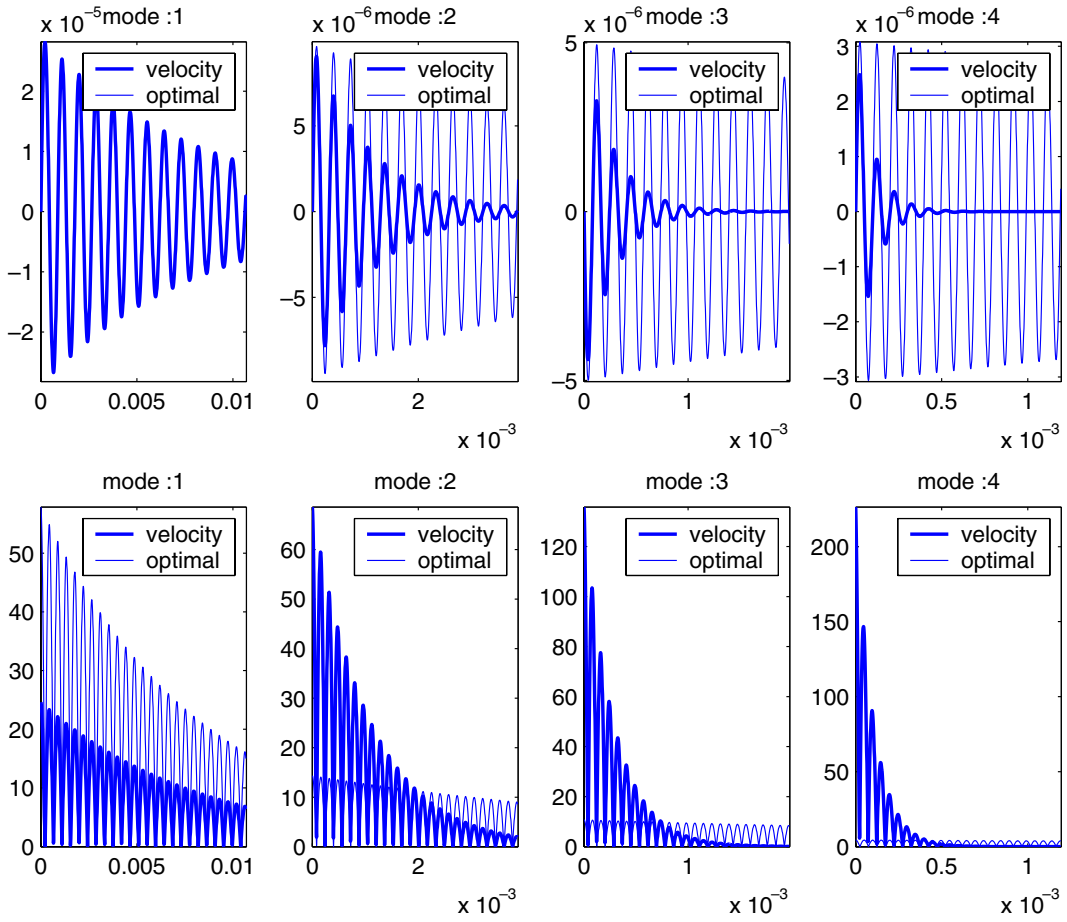

Figure 7. Displacements and voltages for homogenized model.

Table 1. Eigenfrequencies and mode shapes.

Modes	f^{FEM}	f^{Hom}	$\frac{\lvert f_{FEM} - f_{Hom}\rvert}{f_{Hom}}$	$\lVert\psi_n^{Hom} - \psi_n^{FEM}\rVert_{L^2(\Omega)}$	$\lVert\bar{\phi}_n^{Hom} - \bar{\phi}_n^{FEM}\rVert_{L^2(\Omega)}$
1	1.12×10^3	1.13×10^3	6.55×10^{-3}	1.29×10^{-3}	2.01×10^{-2}
2	3.09×10^3	3.11×10^3	6.04×10^{-3}	2.26×10^{-3}	2.27×10^{-3}
3	6.07×10^3	6.10×10^3	5.13×10^{-3}	4.23×10^{-3}	7.19×10^{-1}
4	1.00×10^4	1.01×10^4	3.97×10^{-3}	6.05×10^{-3}	1.03×10^{-1}

Table 2. Decay rates.

Modes	FEM velocity	FEM approx. opt.	Hom. velocity	Hom. optimal
1	−95	−69.9	−120	−120
2	−715	−80.8	−911	−120
3	−2729	−87.5	−3500	−120
4	−6652	−97.7	−9574	−120

Table 3. Energy J.

Modes	FEM velocity	FEM approx. opt.	Hom. velocity	Hom. optimal
1	83	90	79	79
2	145	121	158	93
3	341	182	381	216
4	739	339	834	411

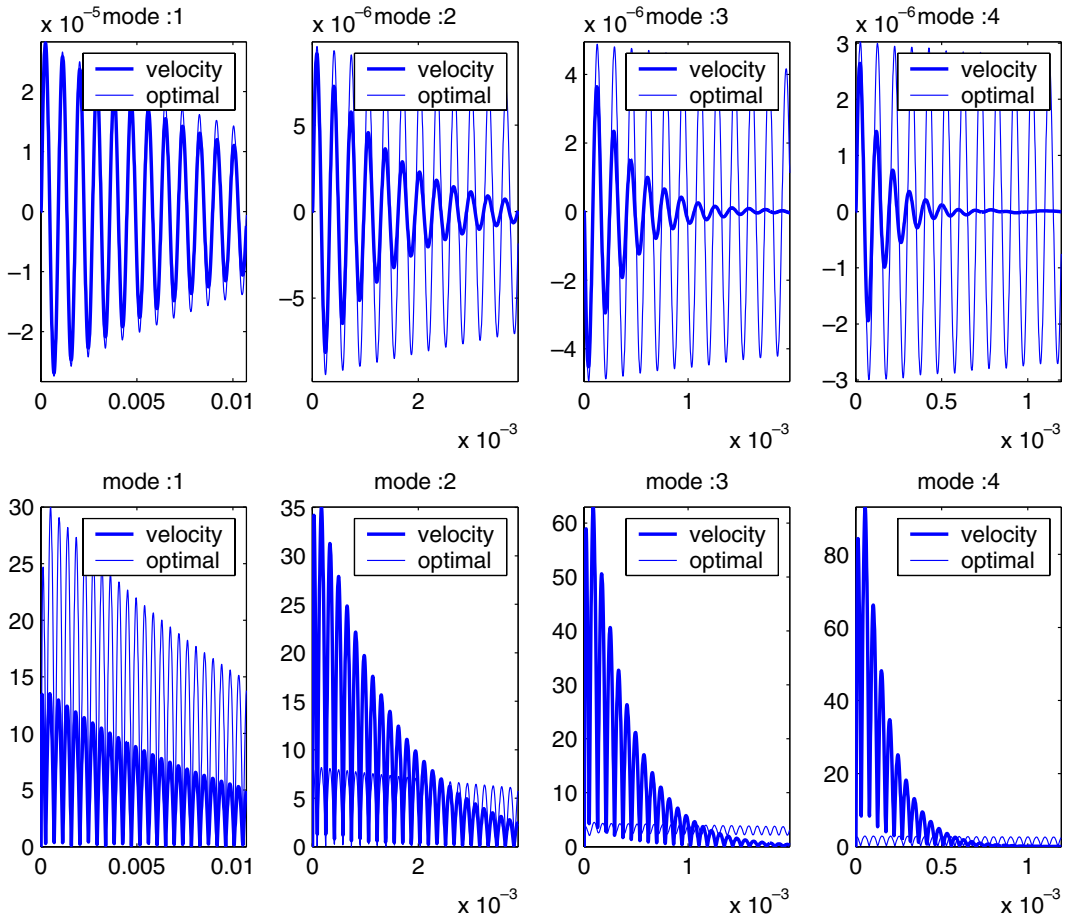

Figure 8. Displacements and voltages for FEM model.

growth. More precisely, it insures the same decay rate of the controlled system solutions at every frequencies (see the fifth column of table 2, which presents the decay rate of solutions for both controls). The value -120 has been chosen arbitrarily, so that voltages remain reasonably low (see their mean values in figure 7 that is described below). In contrast, the decay rates obtained with velocity feedback are much higher for higher modes, which naturally leads to high voltages. These assertions are rigorously true for the homogenized model, on which the control has been synthesized. However, the same tendencies are observed on the FEM model, with relatively high errors due to the various approximations that cannot be discussed here.

Figures 7 and 8 represent evolutions of the mechanical displacements and voltages for both models. The four simulations that are presented for each model correspond to initial conditions proportional to the kth mode, with $k \in \{1, \ldots, 4\}$. Evolution of modes 1, 2, 3 and 4 of mechanical displacements at the respective positions $\xi = \frac{L}{2}, \frac{L}{3}, \frac{L}{4}$ and $\frac{L}{5}$ are represented in the upper parts of the figures. For each mode, twelve periods with velocity feedback and optimal control are superposed. Voltage spatial distributions for modes 1–4, related to velocity feedback and optimal control, are so different (see their representations in the upper and lower parts of figure 6) that it does not make sense to compare voltage evolution for both controllers at a given position. So, evolution of the $L^2(\Omega)$ norm means $\frac{1}{\sqrt{L}}\|\phi\|_{L^2(\Omega)} = \frac{1}{\sqrt{L}}(\int_\Omega |\phi|^2 \,\mathrm{d}\xi)^{1/2}$ is reported in the lower parts of figures 7 and 8. The observations that can be made on these results are just a consequence of those already made on the decay rates. Let us simply remark that the timescale differs for the representation of each mode, which gives the feeling that the decay rates of the optimally controlled solution depend on the mode number.

Now that models have been compared and control results have been discussed, it remains to compare the functional costs $J = \int_0^\infty |Cw|^2 + |Du|^2 \,\mathrm{d}t$ that should be minimized by the optimal control. As predicted, the cost function J is minimized by the optimally controlled solution for both models. Once again, there is quite a large gap between the global solutions of both models.

6. Conclusion

A MIMO LQR control problem, for a given functional, with a large number of distributed inputs and outputs has been addressed for the beam vibration reduction. Without any particular treatment, such a problem should lead to a very large controller that could not be implemented in real time. So, a procedure of approximation, which uses the homogenized model and a high frequency approximation of the Riccati operator, provides a decentralized controller that can be implemented by a distributed analog electrical circuit. Numerical simulations have confirmed the interest in this approach in spite of the predictable approximation

error. Further explorations on stability, robustness, improved approximation of the controller, as well as extensions to other mechanical structures and cost functionals, still remain to be done. Finally, experimental tests using this method remain to be made.

Acknowledgment

I would like to thank the reviewers for their valuable comments, suggestions and corrections.

References

[1] Alecsis http://venus.elfak.ni.ac.yu/∼homer/ealecsis.htm
[2] Bensoussan A, Da Prato G, Delfour M C and Mitter S K 1992 Representation and control of infinite dimensional systems *Systems and Control: Foundation and Application* (Boston, MA: Birkhäuser)
[3] Canon E and Lenczner M 1998 Deux modèles de plaque mince avec inclusions de piézoélectriques et circuits électroniques distribués *C. R. Acad. Sci. Paris, IIb* **326** 793–8
[4] Canon E and Lenczner M 1997 Models of elastics with piezoelectric inclusions. Part I: models without homogenization *Math. Comput. Modelling* **26** 79–106
[5] Curtain R F and Zwart H J 1995 *An Introduction to Infinite-Dimensional Linear System Theory (Springer Text in Applied Mathematics vol 21)* (Berlin: Springer)
[6] Lasiecka I and Triggiani R 1999 Control theory for partial differential equations: continuous and approximation theories *Encyclopedia of Mathematics and its Applications* vol 74 (Cambridge: Cambridge University Press)
[7] Dieulesaint E 1974 *Ondes Élastiques Dans les Solides* (Paris: Masson)